SYNTHESIS OF HYDROXYAPATITE
IN THE PRESENCE OF ANIONIC SURFACTANT

Agnieszka KOLODZIEJCZAK-RADZIMSKA[*]**, Marlena SAMUEL**[*]**,
Dominik PAUKSZTA**[*]**, Adam PIASECKI**[**]**, Teofil JESIONOWSKI**[*]

[*] Poznan University of Technology, Institute of Chemical Technology and Engineering, Faculty of Chemical Technology, M. Skłodowskiej-Curie 2, PL-60-965, Poznan, Poland; e-mail: Agnieszka.Kolodziejczak-Radzimska@put.poznan.pl

[**] Poznan University of Technology, Faculty of Mechanical Engineering and Management, Institute of materials Science and Engineering, Jana Pawła II 24, PL-60-965, Poznan, Poland

Abstract: Hydroxyapatite was synthesized by precipitation method using an anionic surfactant (SDS) template, at ambient temperature and normal pressure. Phosphoric acid and disodium phosphate were used as a precursor of phosphorous, whereas calcium hydroxide and chloride were used as a precursor of calcium. The obtained hydroxyapatite was subjected to a wide range of physicochemical analysis using various measurement techniques. In order to get information about the properties of the obtained products, the following analysis of characteristics was performed: dispersion (NIBS), morphological (SEM), adsorptive (BET) and structural (XRD). Energy-dispersive X-ray spectroscopy and elemental analysis were also applied.

Keywords: hydroxyapatite, precipitation, anionic surfactant

Introduction

Biomaterials belong to a unique materials group. They are distinguishable by their specific composition, structure, and properties. The feature determining their specific character is that they are accepted by the human organism (Cheng, 2010).

Hydroxyapatite (HA) is an interesting example of biomaterials that belong to the apatite group. HA occurs in mineralogical, biological, and synthetic forms (Joschek, 2000; Ferraz, 2004; LeGeros, 2008). Hydroxyapatite is biocompatible, osteoconductive and can easily be processed to matrices with interconnecting pores to allow for no ingrowths (Nunes, 1997). Although it has been reported that HA is almost water insoluble, it is nevertheless biodegradable, though at a very slow rate (Joschek, 2000). In nature, it can be found mainly as a component of metamorphic and

sedimentary rocks, especially in rocks of volcanic origin. Biological hydroxyapatite contains a small amount of fluorine, magnesium and sodium, as well as carbonate and citrate ions (Shi, 2010). Synthetic HA, with the chemical formula of $Ca_{10}(PO_4)_6(OH)_2$, includes hydroxyl groups. The Ca/P ratio in the feed decides whether pure hydroxyapatite and CaO, biphasic calcium phosphate (BCP, HA + β-TCP) or β-tricalcium phosphate ($Ca_3(PO_4)_2$, β-TCP) is formed. The critical Ca/P ratio for which pure hydroxyapatite is obtained is 1.67 (Afshar, 2003; Salma, 2010; Cho, 2011).

The presence of surfactants in a precipitation process influences the dispersion and morphology of obtained products. Numerous reports in the literature have shown that the most widely used surfactants are cationic surfactants (CTAB) (Wang, 2006; Salarian, 2009; Shanti, 2009; Coelho, 2010) or a mixture of cationic/anionic surfactants (CTAB/SDS) (Yan, 2001; Ma, 2011). Therefore, in this study an anionic surfactant (SDS) was used. Sodium dodecyl sulfate (SDS), as one of the macromolecules, is used to control the morphology of HA in aqueous synthetic methods (Tari, 2011). Sodium dodecyl sulfate is an organic compound with the formula $CH_3(CH_2)_{11}OSO_3Na$. It is an anionic surfactant used in many cleaning and hygiene products. The salt is an organosulfate consisting of a 12-carbon tail attached to a sulfate group, giving the material the amphiphilic properties required of a detergent.

The main aim of this work was the synthesis of hydroxyapatite by precipitation method using sodium dodecyl sulfate, SDS. The obtained hydroxyapatite was characterized by dispersive and morphological analysis, BET surface area analysis, and structural, elemental and energy dispersive analysis.

Experimental

Synthesis of hydroxyapatite (HA)

The hydroxyapatite (HA) was obtained in a precipitation process. The process was performed in a reactor of 0.5 dm^3 capacity, equipped with a fast-rotating stirrer (Eurostar digital IKA–Werke GmbH, 1200 obr/min). In the first stage, a reactor was charged with a solution containing PO_4^{3-} ions (H_3PO_4 or Na_2HPO_4 from Sigma-Aldrich) and anionic surfactant (SDS from Sigma-Aldrich). The mixture was intensively stirred for about 15 min. The pH was adjusted to 12 with 1N NaOH. In the second stage, the solution containing Ca^{2+} ions ($Ca(OH)_2$ or $CaCl_2$ from Sigma-Aldrich) was dosed using an Ismatec ISM833A type peristaltic pump at the rate of 2 cm^3/min, into a reactor. A white milky solution was obtained. After 24 h of aging, the solution was filtered along with repeated washing to remove residues of the surfactant. Then the filtrate cake was dried out.

Table 1. Experimental conditions of the precipitation process

Sample symbols	Source of Ca^{2+} ions	Concentration of Ca^{2+} ions [M]	Source of PO_4^{3-} ions	Concentration of PO_4^{3-} ions [M]	Concentration of SDS [g]
HA0	CaCl$_2$		H$_3$PO$_4$		–
HA0'			Na$_2$HPO$_4$		
HA1	Ca(OH)$_2$	1	H$_3$PO$_4$	0.6	
HA2	CaCl$_2$				0.8
HA3	Ca(OH)$_2$		Na$_2$HPO$_4$		
HA4	CaCl$_2$				

Four samples, labelled as HA1, HA2, HA3 and HA4 were obtained. Table 1 presents the conditions of precipitation and main data of the samples, while Figure 1 shows the schema for obtaining hydroxyapatite from the precipitation method.
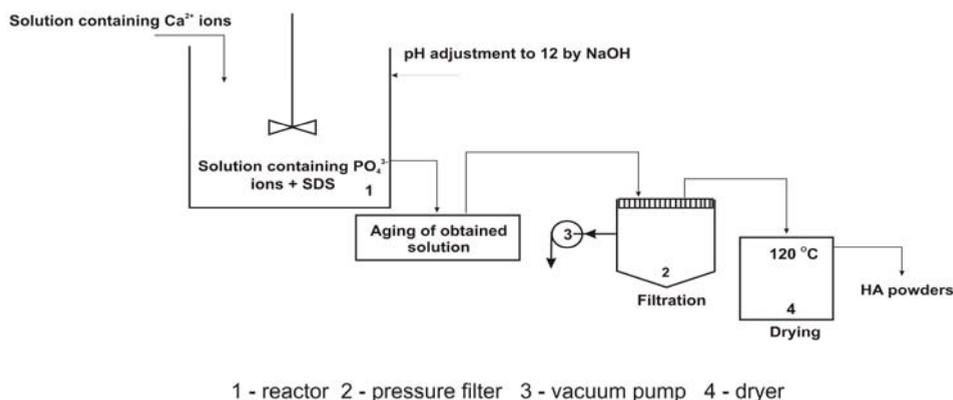

Fig. 1. Preparation of hydroxyapatite – a schematic presentation

Physicochemical evaluation

The dispersive characteristics of obtained hydroxyapatite samples were determined by using an a Zetasizer Nano ZS and Mastersizer 2000, both made by Malvern Instruments Ltd., operating on the non-invasive back-scattering method and laser diffraction method measuring particles of sizes ranging from 0.6 to 6000 nm and from 0.2 to 2000 μm, respectively. Measurements of particle size were repeated at least ten times for each sample. At the next stage, the morphology and microstructure of hydroxyapatite were investigated using a Zeiss EVO40 Scanning Electron Microscope. In order to characterise the adsorption properties, nitrogen adsorption/desorption isotherms at 77 K and parameters such as surface area (A_{BET}), total volume (V_p) and mean size (S_p) of pores were determined using an ASAP 2020 instrument (Micromeritics Instrument Co.). All samples were degassed at 120 °C for

4 h prior to measurement. The surface area was determined by the multipoint BET (Brunauer-Emmett-Teller) method using the adsorption data as a function of relative pressure (p/p_0). The BJH (Barrett-Joyner-Halenda) algorithm was applied to determine the total pore volume and the average pore size. The crystalline structure of individual samples was resolved using the X-ray diffraction method. The diffractograms were recorded using a TUR-M-62 horizontal diffractometer, equipped with HZG-3 type goniometer. To obtain the radiation intensity distribution curve $I = f(\theta)$, a counting rate gauge interoperated with the counter and electronically coupled to a graphic recorder was used. Moreover, the surface composition of hydroxyapatite (contents of Ca and P) was analyzed by energy dispersive X-ray spectroscopy (EDS) using a Princeton Gamma-Tech unit equipped with a prism digital spectrometer. EDS technique is based on an analysis of X-ray energy values using a semiconductor. Before the analysis, the sample was placed on the ground with a carbon paste or tape. The presence of carbon materials is needed to create a conductive layer, which ensures the delivery of electric charge from the sample. Representative parts (500 μm^2) were analyzed for proper surface composition evaluation.

Results and discussion

Dispersive and morphological characteristic

Figure 2 presents particle size distributions of obtained hydroxyapatite without and in the presence of SDS, using different initial substrates. Analyzing the presented distribution curves, it was found that hydroxyapatite precipitated without SDS characterized by higher particles in relation to the HA samples precipitated in presence of SDS. In this case, the obtained samples were characterized by particles above 1000 nm. The maximum diameter (close to 20% for sample HA0 and 10% for HA0') came from particles of 4600 nm (HA0) and 2300 nm (HA0'). Hydroxyapatite samples precipitated from calcium hydroxide characterized by significantly smaller particles in relation to the HA samples precipitated from calcium chloride. The smallest particles were obtained for HA3 samples (hydroxyapatite precipitated from $Ca(OH)_2$ and Na_2HPO_4). In this case, the obtained particles have a diameter in the range of 78–164 nm, where the maximum diameter (close to 34%) came from particles of 106 nm diameter. Results of the analysis, obtained from Mastersizer 2000, revealed that in sample HA3 10% of particles [d(0.1)] have diameter not greater than 3.29 μm, 50% of particles [d(0.5)] have diameter not greater than 18.53 μm, and 90% [d(0.9)] have diameters not greater than 52.69 μm. The mean diameter of particles in this sample [D[4.3]] equals to 23.90 μm. The hydroxyapatite precipitated as the HA1 sample (obtained from $Ca(OH)_2$ and H_3PO_4) contains minimal greater size of particles (106–220 nm). In this sample, the maximum volume contribution of about 36.6% came from particles of 142 nm diameter. According to the micrometric particles size (Table 2), the sample contains 90% of particles of diameters smaller than 46.49 μm, 50% of particles have diameter of 22.23 μm, and 10% of particles of diameters not greater

than 6.88 μm. The mean diameter of particles in this sample [D[4.3]] equals to 24.85 μm. However when $CaCl_2$ (Figs 2b, d, Table 2) is used as a source of calcium ionic, we obtain particles in the significantly larger size, and an agglomerate occurs above 1000 nm. The hydroxyapatite precipitated as a HA2 had diameters in the range 1280–2300 nm, and the maximum volume contribution of about 34% came from particles of 1720 nm diameter. In addition, the micromeritic particles (for HA2 and HA4 samples) have the higher sizes. The SEM images of the particles morphology of HA1 (obtained from $CaCl_2$ and H_3PO_4) and HA3 (obtained from $CaCl_3$ and Na_2HPO_4) samples show that they are characterized by a greater homogeneity, compared to the samples precipitated as a HA2 and HA4 (Fig. 2). In interpreting the SEM images of HA1 and HA3 samples, we can also see that this hydroxyapatite sample demonstrates (displays) a tendency to create agglomerates.

Comparing our results with the literature data, we can say that using a different surfactant, particles of HA of various structure and size can be obtained. Liu et al. (2004) synthesized HA nanorods of 50–80 nm in diameter and 0.5–1.2 μm in length using surfactants of CTAB and PEG 400. Shanti et al. (2009) obtained hydroxyapatite rods with diameter 20 nm and length in the range of 100–120 μm using only cationic surfactant (CTAB). Yan et al. (2001) used an anionic surfactant (SDS) as regulator of the nucleation and crystal growth in the synthetic method of preparing HA. The obtained hydroxyapatite had particles of nanorods structure (150 nm/10 nm).

Table 2. Dispersive characteristics of obtained hydroxapatite

Sample number	Zetasizer Nano ZS		Mastersizer 2000			
	Particle diameter (nm)	Polidyspersity index (PdI)	Particle diameter (μm)			
			d(0.1)	d(0.5)	d(0.9)	D[4.3]
HA0	68–122 3090–6440	0.734	5.88	37.44	80.91	41.12
HA0'	1110–3580	0.395	5.02	40.75	92.38	45.40
HA1	106–220	0.393	6.88	22.23	46.49	24.85
HA2	1280–2300	0.491	4.41	38.92	89.88	33.37
HA3	98–164	0.436	3.29	18.53	52.69	23.90
HA4	396–1110	0.232	3.94	33.18	85.06	39.36

X-Ray diffraction

The XRD pattern of the synthesized sample in the presence of SDS is shown in Fig. 3. From the XRD pattern, we can say that in all cases there is only HA. Four intensive peaks are located in $2\theta = 25.9°$ (002), $2\theta = 31.5$ (211), $2\theta = 32.2$ (112) and $2\theta = 32.7$ (300), which indicate the high crystallinity of HA particles. Phase identification of the synthesized powders was accomplished by comparing the experimental XRD patterns with the database compiled by the Joint Committee on Powder Diffraction Standards (JCPDS), namely the following card number: 9-432 for $Ca_{10}(PO_4)_6(OH)_2$ (Salarian, 2009). Our observations are in agreement with previous research (Tari, 2011; Yan, 2001; Yu, 2011).
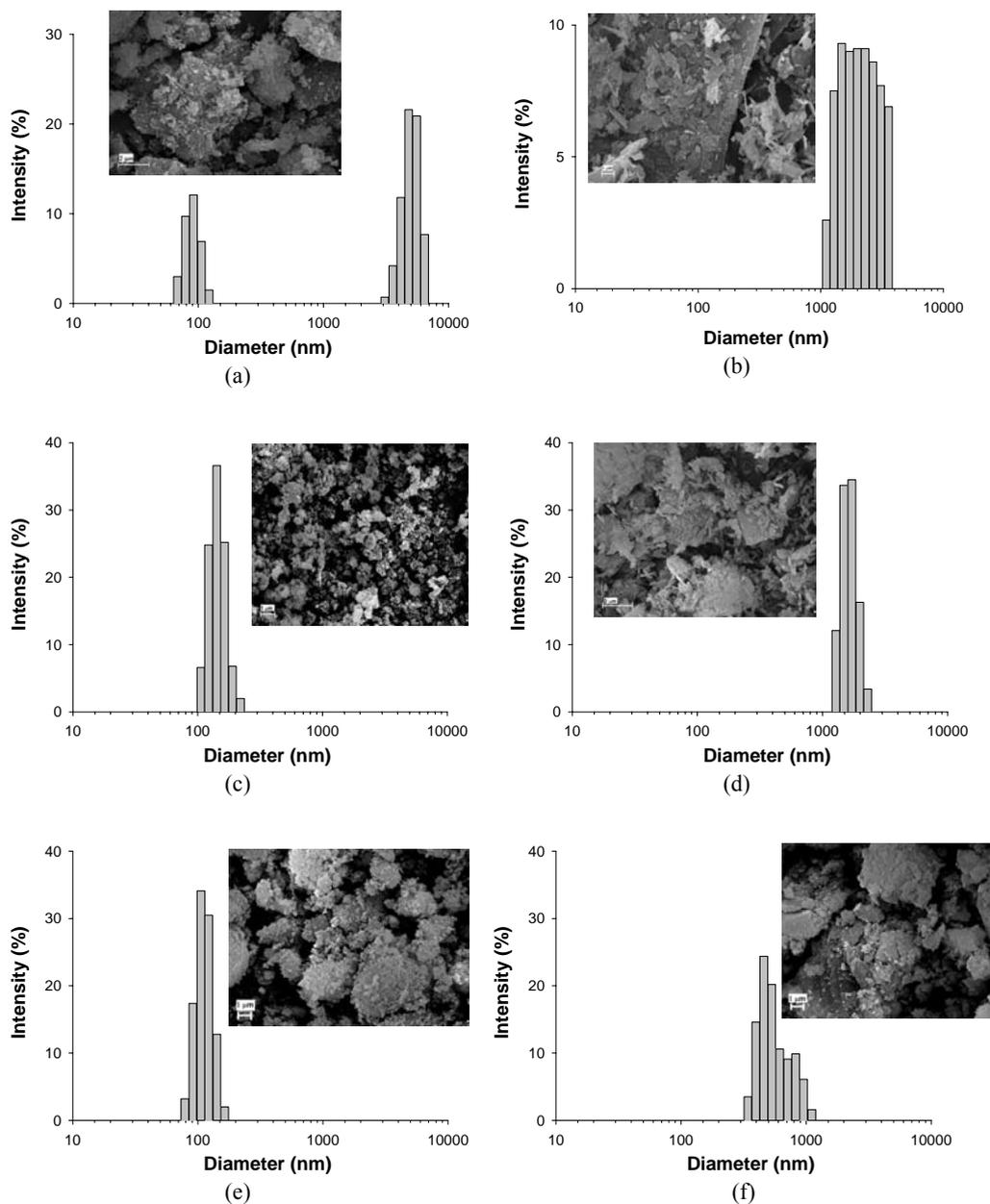
(a)

(b)

(c)

(d)

(e)

(f)

Fig. 2. Particle size distribution (Zetasizer Nano ZS) and SEM microphotographs of hydroxyapatite obtained from different compounds: (a) HA0 – $CaCl_2$, H_3PO_4 without SDS; (b) HA0' – $CaCl_2$, Na_2HPO_4 without SDS; (c) HA1 – $Ca(OH)_2$, H_3PO_4; (d) HA2 – $CaCl_2$, H_3PO_4; (e) HA3 – $Ca(OH)_2$, Na_2HPO_4; (f) HA4 – $CaCl_2$, Na_2HPO_4
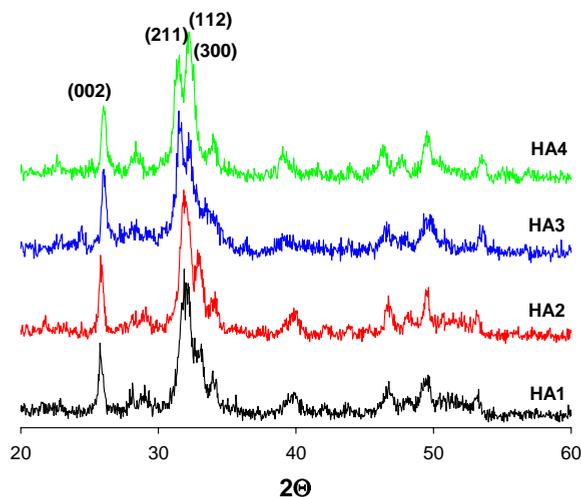
Fig. 3. XRD diffraction patterns of hydroxyapatite structures

Element	Mass contribution (%)	Ca/P ratio (-)
Ca	64.75	1.84
P	35.25	

(a)

Element	Mass contribution (%)	Ca/P ratio (-)
Ca	61.10	1.57
P	38.90	

(b)

Element	Mass contribution (%)	Ca/P ratio (-)
Ca	63.54	1.74
P	36.46	

(c)

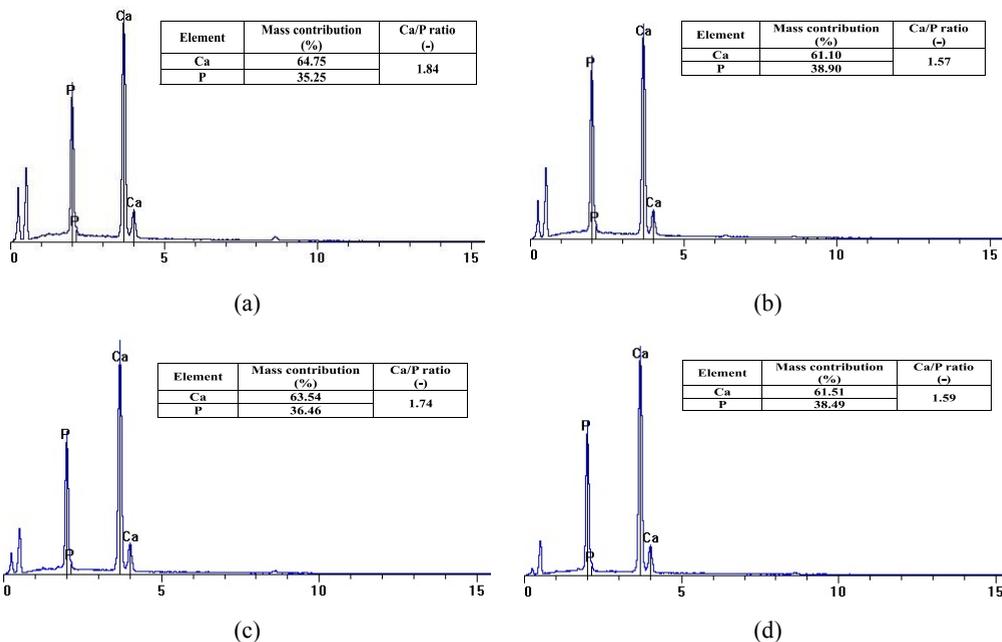| Element	Mass contribution (%)	Ca/P ratio (-)
Ca	61.51	1.59
P	38.49	

(d)

Fig. 4. Energy dispersive spectroscopy (EDS) analysis of hydroxyapatite samples:
(a) HA1, (b) HA2, (c) HA3 and d) HA4

Energy dispersive characterization

The Ca/P ratio in the obtained HA was calculated based on the content of Ca and P. Energy dispersive spectroscopy (EDS) analysis of the products (Fig. 4) shows that the

Ca/P ratio is 1.59–1.84:1. The Ca/P ratio in the HA2 and HA4 samples is in the range 1.5–1.67 and is most similar to the stoichiometric hydroxyapatite (1.67). Whereas, the HA1 and HA3 samples are characterized by the Ca/P ratio 1.74–1.84, which indicates the presence of hydroxyapatite with an excess of calcium. Josheck et al. (2000) and Ooi et al (2007) observed analogous results.

Elemental analysis

In order to determine the degree elute of the surfactant from the obtained hydroxyapatite samples, an elemental analysis was performed. This analysis enables one to determine the carbon, hydrogen and sulfur amount. Analyzing the data presented in Table 3, a small amount of sulfur (< 0.05%) was determined, which may indicate a sufficient washing of the samples.

Table 3. Elemental content of the hydroxyapatite samples obtained in presence of SDS

Sample number	C	H	S
	(%)		
HA1	0.64	0.69	0.04
HA2	0.26	0.82	0.05
HA3	1.23	0.57	0.04
HA4	0.27	0.54	0.04

Characteristics of porous structure of obtained hydroxyapatite

Nitrogen adsorption/desorption isotherms and pore size distributions of the obtained hydroxyapatite samples (HA1 and HA3) are shown in Figure 5. The isotherms were classified as type IV and the hysteresis loops as type H3, which points to the mesoporous structure of the HA samples. A type IV isotherm is related to capillary condensation taking place in mesopores. As can be seen in Table 4, the HA samples obtained in the presence of SDS has the largest specific surface areas in comparison with samples obtained without SDS, the largest (115.1 m^2/g) being recorded for sample HA3. The pore volume and mean pore diameter in this sample were 0.502 cm^3/g and 17.4 nm respectively. The smallest specific surface area (30.9 m^2/g) was determined for sample HA2 (Table 4), and the pore volume and mean pore diameter in this sample were 0. 021 cm^3/g and 2.8 nm. The specific surface areas of sample HA1 and sample HA4 (Table 2) were 84.0 and 83.5 m^2/g, while their pore volumes were 0.270 and 0.057 cm^3/g and the mean pore diameters 12.9 and 2.7 nm, respectively. From analysis of the parameters of the HA precipitation process, it can be concluded that with an increase in the size of particles diameter there is a decrease in the specific surface area of the resulting samples.

Table 4. Characteristics of porous structure of obtained hydroxyapatite

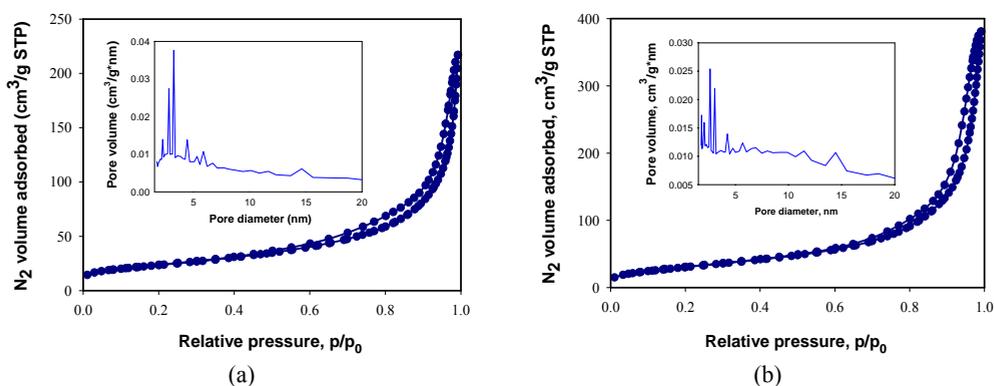| Sample number	Specific surface area (m^2/g)	Pore volume (cm^3/g)	Pore diameter (nm)
HA0	20.4	0,015	2.8
HA0'	17.7	0.012	2.8
HA1	84.0	0.270	12.9
HA2	30.9	0.021	2.8
HA3	115.1	0.502	17.4
HA4	83.5	0.057	2.7

Fig. 5. Nitrogen adsorption/desorption isotherms and pore size distributions
of hydroxyapatite samples a) HA1 and b) HA3

Figure 6 presents a probable mechanism for the formation of hydroxyapatite particles in the compositions containing the anionic surfactant. Earlier studies show that the sulfate groups are able to interact with calcium ions present in an aqueous solution. Surfactant molecules in micelles or as emulsion droplets interact with C^{2+} ions to form zwitterions (Zhao, 2009). These numerous calcium-rich domains lead to the rapid formation of HA particles on contact with phosphate in the aqueous phase. In addition, the positional stabilization of Ca^{2+} ions within each zwitterions structure as a result of the electrostatic interaction effect by SDS molecules favours the formation of ordered HA crystals (Tari, 2011).
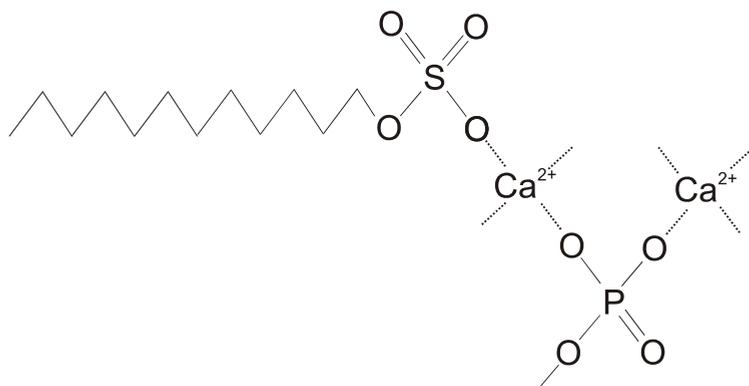
Fig. 6. A schematic drawing showing the interaction
between the surfactant anion and calcium cation (Tari, 2011)

Conclusions

Crystalline hydroxyapatite was successfully prepared by adding anionic surfactant at ambient temperature and normal pressure. The XRD studies confirm the pure crystalline structure of HA. The investigated dispersive-morphological research shows that hydroxyapatite obtained from hydroxide calcium and disodium phosphate (sample HA3) is characterized by the smallest particles. Their diameters varied in the range from 78-164 nm and have regular structure. Additionally, the largest specific surface area was observed (115.1 m^2/g) for this sample. The greatest size particles were obtained in sample HA2; their diameters varied in a range from 1280-2300 nm. This sample is also characterized by the smallest specific surface area (30.9 m^2/g). The maximum volume contribution (close to 34%) came from particles of 1720 nm diameter. Energy dispersive analysis showed that the obtained hydroxyapatite samples are characterized by Ca/P ratio in the range of 1.59-1.84. This range indicates that some of the HA samples contain excess calcium. The small amount of the sulfur (0.05%) in the obtained HA samples points to sufficient washing of the surfactants residue.

Acknowledgements

References

AFSHAR A., GHORBANI M., EHSANI N., SAERI M.R., SORRELL C.C., 2003, *Some important factors in the wet precipitation process of hydroxyapatite*, Materials and Design, 24, 197–202.

CHENG, H.N., GROSS R.A., 2010, *Green polymer chemistry: biocatalysis and biomaterials*, ACS Symposium Series, American Chemical Society, Washington, DC, Chapter 1, 1–14.

CHO J.S., RHEE S.H., 2011, *The densification mechanism of hydroxyapatite particles during spray pyrolysis with variable carrier gas rates of flow*, Journal of Biomedical Materials Research B: Applied Biomaterials, 2, 493–500.

COELHO J.M., MOREIRA J.A., ALMEIDA A., MONTEIRO F.J., 2010, *Synthesis and characterization of HAp nanorods from a cationic surfactant template method*, Journal of Materials Science: Materials in Medicine, 21, 2543–2549.

FERRAZ M.P., MONTEIRO F.J., MANUEL C.M., 2004, *Hydroxyapatite nanoparticles: a review of preparation methodologies*, Journal of Applied Biomaterials & Biomechanics, 2, 74–80.

JOSCHEK S., NIES B., KROTZ R., GOPFERICH A., 2000, *Chemical and physicochemical characterization of porous hydroxyapatite ceramics made of natural bone*, Biomaterials, 21, 1645–1658.

LIU Y., HOU D., WANG G., 2004, *A simple wet chemical synthesis and characterization of hydroxyapatite nanorods*, Material Chemistry and Physics, 86, 69–73.

MA T., XIA Z., LIAO L., 2011, *Effect of reaction system and surfactant additives on the morphology evolution of hydroxyapatite nanorods obtained via a hydrothermal route*, Applied Surface Science, 257, 4384–4388.

NUNES C.R., SIMSKE S.J., SACHADEVA R., WOLDORD L.M., 1997, *Long-term ingrowth and apposition of porous hydroxyapatite implants*, Journal of Biomedical Material Research, 36, 560–563.

LEGEROS R.Z., 2008, *Calcium phosphate-based osteoinductive materials*, Chemical Reviews, 108, 4742–4753.

OOI C.Y., Hamdi M., RAMESH S., 2007, *Properties of hydroxyapatite produced by annealing of bovine bone*, Ceramics International, 33, 1171–1177.

SADAT-SHOJAI M., KHORASANI M.-T., DINPANAH-KHOSHDARGI E., JAMSHIDI A., 2013, *Synthesis methods for nanosized hydroxyapatite with diverse structures*, Acta Biomaterialia, 9, 7591–7621.

SALARIAN M., SOLATI-HASHJIN, SHAFIEI S.S., GOUDARZI A., SALARIAN R., NEMATI A., 2009, *Surfactant-assisted synthesis and characterization of hydroxyapatite nanorods under hydrothermal conditions*, Materials Science-Poland, 27, 961–972.

SALMA K., BERZINA-CIMDINA L., BORODAJENKO N., 2010, *Calcium phosphate bioceramics prepared from wet chemically precipitated powders*, Processing and Application of Ceramics, 4, 45–51.

SHANTI P.M.S.L., ASHOK M., BALASUBRAMANIAN T., RIYASDEEN A., AKBARSHA M.A., 2009, *Synthesis and characterization of nan-hydroxyapatite at ambient temperature using cationic surfactant*, Materials Letters, 63, 2123–2125.

SHI D., 2004, *Biomaterials and tissue engineering*, Springer Berling Heidelberg, Germany

TARI N.E., MOTLAGH M.M.K., SOHRABI B., 2011, *Synthesis of hydroxyapatite particles in cationic mixed surfactants template*, Materials Chemistry and Physics, 131, 132–135.

WANG Y.J., CHEN J.D., WEI K., ZHANG S.H., WANG X.D., 2006, *Surfactant-assisted synthesis of hydroxyapatite particles*, Materials Letters, 60, 3227–3231.

WANG Y., ZHANG S, WEI K, ZHAO N., CHEN J., WANG X., 2006, *Hydrothermal synthesis of hydroxyapatite nanopowders using cationic surfactant as a template*, Materials Letters, 60, 1484–1487.

YAN L., LI Y., DENG Z.X., ZHUANG J., SUN X., 2001, *Surfactant-assisted hydrothermal synthesis of hydroxyapatite nanorods*, International Journal of Inorganic Materials, 3, 633–637.

YU G., SHAO W., 2011, *Synthesis of hydroxyapatite assisted by surfactants*, 4th International Conference on Biomedical Engineering and Informatics (BMEI), 1260–1263.

ZHAO J., LIU J., JIANG J., 2009, *Interaction between anionic and cationic gemni surfactants at air/water interface and in aqueous bulk solution*, Colloids and Surfaces A: Physicochemical and Engineering Aspects, 350, 141–146.